VERSITA

Cent. Eur. J. Chem. • 9(4) • 2011 • 624-634
DOI: 10.2478/s11532-011-0043-5

Central European Journal of **Chemistry**

Spectral study of coumarin-3-carboxylic acid interaction with human and bovine serum albumins

Research Article

Aurica Varlan, Mihaela Hillebrand*

Department of Physical Chemistry, University of Bucharest, Bucharest 030016, Romania

Received 17 November 2010; Accepted 4 March 2011

Abstract: Fluorescence spectroscopy and circular dichroism (CD) spectroscopy were used to investigate the interaction of coumarin-3-carboxylic acid with human serum albumin (HSA) and bovine serum albumin (BSA) under physiological conditions in a buffer solution of pH 7.4.

Quenching constants were determined using the Lineweaver-Burk equation to provide a measure of the binding affinity of coumarin-3-carboxylic acid to HSA/BSA. Binding studies concerning the number of binding sites, n, and apparent binding constant, *K*, were performed by a fluorescence quenching method at different temperatures (298, 303 and 310 K). The thermodynamic parameters, enthalpy change (ΔH^0) and entropy change (ΔS^0) as calculated according to the van't Hoff equation, indicated that hydrogen bonding and van der Waals forces play a major role in coumarin-3-carboxylic acid-HSA association whereas electrostatic interactions dominate in coumarin-3-carboxylic acid-BSA association. The distance, r, between the donor (HSA/BSA) and acceptor (coumarin-3-carboxylic acid) has been estimated using Förster's equation, on the basis of resonance energy transfer. Furthermore, CD spectra were used to investigate the α-helix changes of the HSA and BSA molecules upon addition of coumarin-3-carboxylic acid.

Keywords: *Human Serum Albumin • Bovine Serum Albumin • Coumarin-3-carboxylic acid • Fluorescence quenching • Circular dichroism*

1. Introduction

The binding ability of a drug to the serum albumin in blood may have a considerable impact on the distribution, free concentration and metabolism of the drug. Binding parameters are, thus, helpful in the study of pharmacokinetics and the design of dosage forms [1,2].

Human serum albumin (HSA), the most prominent protein in plasma, has the capability to bind a wide range of endogenous and exogenous compounds such as nonesterified fatty acids, heme, bilirubin, thyroxine, and bile acids, as well as an extraordinarily broad range of drugs [3-7]. Bovine serum albumin (BSA) is used as a standard as it can be isolated in a highly pure form. Moreover, BSA is highly stable and comparatively cheap.

Coumarin (chromen-2-one) establishes a family of dyes [8–10] that are applicable in different fields of science and technology. Coumarin and their derivatives have been a subject of considerable interest in numerous fields [11–13]. They exhibit strong fluorescence in the UV–VIS region that makes them suitable to use as colorants, dye laser media and nonlinear optical chromophores.

The bioactivity of coumarin and more complex related derivatives appears to be based on the coumarin fragment [14-16]. Biological effects observed include anti-bacterial [17], anti-thrombotic and vasodilatory [18] and anti-tumourigenic. Coumarin derivatives are used as fluorescent indicators of a region's pH and as fluorescent probes to determine the rigidity and fluidity of a living cell and its surrounding medium. Among coumarins, coumarin-3-carboxylic acid (I) (Fig. 1) has an important chemotherapeutic potential [19]. Moreover, due to its pKa value of 3.28 (data not shown), at the optimum pH = 7.4 used for the proteins, it will be in the dissociated form, enhancing the possibility of electrostatic interactions.

The interesting properties associated with coumarins motivated us for the present investigation, continuing our previous work on other heteroaromatic carboxylic ligand-albumin interactions [20,21].

* *E-mail: mihh@gw-chimie.math.unibuc.ro*
mihaela.hillebrand@gmail.com

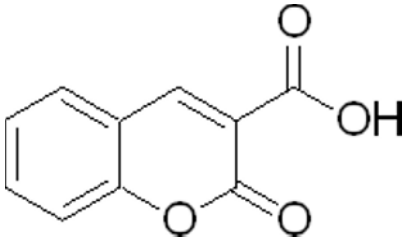

Figure 1. The structure of coumarin-3-carboxylic acid, (I)

2. Experimental Procedure

2.1. Materials

Bovine serum albumin (BSA, Fraction V, approximately 99%), human serum albumin (HSA, fatty acid free < 0.05%) and coumarin-3-carboxylic acid were purchased from Sigma Chemical Company, St Louis, USA. The solutions of coumarin-3-carboxylic acid, BSA and HSA were prepared in pH 7.4 phosphate buffer; the protein solutions were equilibrated over night and kept in the dark. As the pKa of coumarin-3-carboxylic acid is 3.28, at pH=7.4 we can consider the acid-base equilibrium totally shifted towards the carboxylate form.

2.2. Apparatus and methods

Fluorescence measurements were made on Jasco FP-6300 spectrofluorimeter, using a quartz cell of 1 cm path length. Both the excitation and emission slits were set at 5.0 nm. Fluorescence spectra were recorded at three different temperatures (298, 303 and 310 K) in the wavelength range of 300–550 nm, after exciting HSA or BSA at 286 nm. A thermostat water-bath from Lauda was used for controlling the temperature.

CD measurements were made on a Jasco J-815 CD spectrometer using a 1.00 cm cell at 0.2 nm intervals, with three scans averaged for each CD spectrum in the range 200–260 nm. Results are expressed as ellipticity (θ) in millidegrees.

Time-resolved fluorescence decays were recorded in a time-correlated single photon counting FLS920 system from Edinburgh Instruments, with excitation at 304 nm. The data were fitted with a multiexponential decay and χ^2 was less than 1.060. Average lifetimes were calculated according to [22].

Measurements were made monitoring the changes of the intrinsic properties of albumins (intrinsic fluorescence at 346/339 nm, and the negative CD signal at 208-220 nm) upon increasing the ligand concentrations. On the basis of preliminary experiments, HSA and BSA concentrations were kept fixed at 0.75×10^{-6} M and the drug concentrations were varied to ensure a dye to polymer ratio, d/p, in the range 0 – 8.03. At these low concentrations, in spite of the extinction coefficient of the ligand at the excitation wavelength ($\varepsilon_{300}\approx10000$ $M^{-1}cm^{-1}$), the inner filter effect was insignificant even for the higher d/p used. The value of the d/p ratio was sufficient to describe the fluorescence quenching process well while avoiding solubility problems.

In order to have an insight on the possible location of the coumarin-carboxylate ion, the experiments were also conducted in the presence of warfarin and ibuprofen, known markers for sites I and II, respectively; aliquots of the ligand were added to a solution containing equimolar concentrations (0.75 μM) of albumin and markers.

3. Results and Discussions

3.1. The fluorescence quenching mechanism

The fluorescence spectra of the albumins in the presence of increasing concentration of (**I**) are presented in Figs. 2A and 2B and reflect the quenching of the intrinsic fluorescence of albumin.

Fluorescence quenching could proceed *via* different mechanisms, usually classified as dynamic and static quenching. Increasing temperature is likely to result in decreased stability of complexes, and thus lower values of the static quenching constants.

The steady state fluorescence spectra were first analyzed in terms of the Stern Volmer equation, Eq. 1:

$$F_0/F=1+K_{SV}[Q] \quad (1)$$

where F_0 and F denote the steady-state fluorescence intensities in the absence and in the presence of quencher (the coumarin-3-carboxylate ion), respectively, K_{SV} is the Stern-Volmer quenching constant, and *[Q]* is the concentration of the quencher.

The Stern–Volmer plots at three temperatures (298, 303, and 310 K) are presented in Figs. 3A and 3B, and the corresponding constants are given in Table 1. For both albumins, at 0.75 μM concentration, the plots are linear with slopes decreasing with increasing temperature, indicating a predominant static quenching mechanism.

Moreover, the calculation of the bimolecular rate constant, k_q using Eq. 2:

$$k_q = K_{SV} / \tau_0 \quad (2)$$

where τ_0 is the average lifetime of the protein without the quencher (10^{-8}s, [22]) led to 5.77×10^{12} $M^{-1}s^{-1}$ for HSA and 6.47×10^{12} $M^{-1}s^{-1}$ for BSA, both values larger than the maximum scatter collision quenching constant of the biomolecule ($k_q = 2.0\times10^{10}$ M^{-1} s^{-1}) [23].

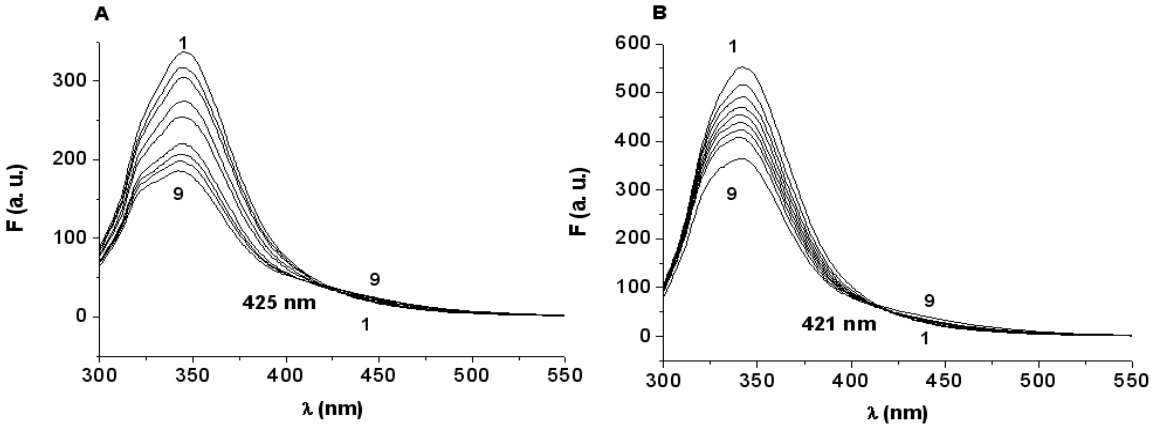

Figure 2. Emission spectra of A) [HSA] = 0.75×10^{-6} M, λ_{ex} = 286 nm, λ_{em} = 346 nm; B) [BSA] = 0.75×10^{-6} M, λ_{ex} = 286 nm, λ_{em} = 339 nm; 1–9: d/p = 0; 0.44; 1.31; 1.73; 2.99; 3.40; 4.61; 6.17; 8.03; pH 7.4, T=298 K.

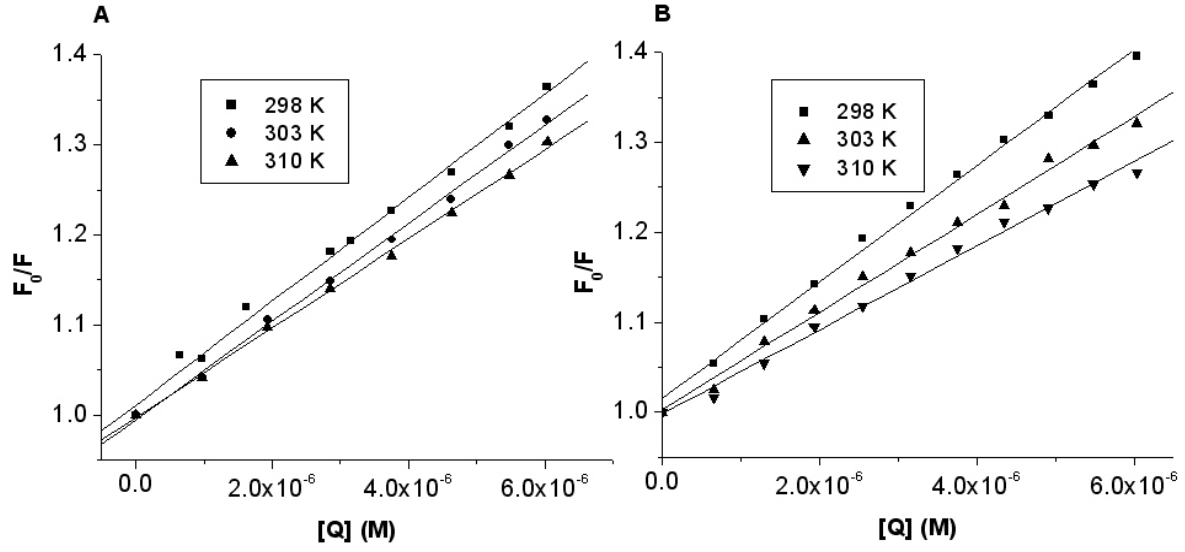

Figure 3. Stern-Volmer plots at different temperatures for A) [HSA]= 0.75×10^{-6} (M); B) [BSA]= 0.75×10^{-6} (M); d/p=0-8.03; pH 7.4.

Fluorescence lifetime analysis was used to differentiate between static and dynamic quenching [24] (Fig. 4).

In order to determine the SV constant corresponding to dynamic quenching, lifetime measurements for the proteins and protein-ligand mixtures were performed. The decays were triexponential and the three components, 1.04 ns (5.3%), 4.61 ns (49.2%), 8.14 ns (45.5%) (χ^2 = 1.060) and average lifetimes for HSA (6.02 ns) are in good agreement with literature data [25]. The dynamic SV constant is K_{SV} = (4.6±0.6)×10^3 M^{-1} (R= 0.998) for BSA and (3.4±0.1)×10^3 M^{-1} (R = 0.990) for HSA, about one order lower than that determined from steady-state measurements, confirming the predominance of the static quenching mechanism due to protein-ligand binding. Therefore, considering the linear shape of the steady state SV plots in the range of the concentrations used, and that the corresponding constants override the value of the dynamic contribution, we have neglected the latter in the following analysis.

The static quenching constants were further determined using the Lineweaver-Burk equation [26,27]:

$$(F_0\text{-}F)^{-1} = F_0^{-1} + K_{LB}^{-1} F_0^{-1} [Q]^{-1} \quad (3)$$

where K_{LB} (M^{-1}) is the static quenching constant, which describes the binding efficiency of micromolecules to biological macromolecules at ground state. The plots are displayed in Figs. 5A and 5B, and the constants are also listed in Table 1.

3.1.1. Binding constant and the binding sites

Several models are given in the literature for the determination of the binding parameters, the number of sites and the binding constants, considering one or

several classes of binding. Generally, all the models start from the Scatchard equation [28] for a single class of *n* independent binding sites, Eq. 4:

$$\nu = \frac{n \times K \times [L_f]}{(1 + K \times [L_f])} \quad (4)$$

where ν represents the binding ratio, *i.e.*, the ratio of the bound ligand concentration, *[L$_b$]*, to the total protein concentration *[P$_t$]*, *[L$_f$]* is the concentration of the free ligand at equilibrium, *K* is the association constant and *n* the number of binding sites. Working on the protein band, the calculation of ν is made considering that the measured fluorescence, *F*, at a given ligand concentration, is due to the unbound protein concentration, *[P]*:

$$\frac{F_0}{F} = \frac{[P_t]}{[P]} \quad (5)$$

$$\nu = \frac{[L_b]}{[P_t]} = \frac{[L_t] - [L_f]}{[P_t]} = n \times \frac{[P_t] - [P]}{[P_t]} = n \times \frac{(F_0 - F)}{F_0} \quad (6)$$

where F_0 and *F* denotes the steady-state fluorescence intensities in the absence and in the presence of quencher.

The main problem of the Scatchard equation is that in some models, the free ligand concentration, *[L$_f$]* is replaced by the total concentration, *i.e.*, by the amount of the added ligand, *[L$_f$] = [L$_t$]*, an approximation which is not always valid. In the following, in order to rationalize our experimental data on the albumin−coumarin-3-carboxylic acid systems, we have focused on Eq. 7, in which such approximations are avoided.

$$log \frac{F_0 - F}{F} = n \times log\, K - n \times log \frac{1}{[L_t] - \frac{F_0 - F}{F_0} \times [P_t]} \quad (7)$$

where all the symbols have the same meaning as previously discussed.

The slope of the linear plot of *log (F$_0$-F)/F* vs. *log (1/([L$_t$] –(F$_0$-F) × [P$_t$]/F$_0$))*, Eq. 7, gives the number of sites, and the intercept with the ordinate is the product *n×log K* (Figs. 6A and 6B).

Recently [29], considering that the ligand protein complex is not totally nonfluorescent, a correction of this equation was suggested. In our case, using the modified equation, the differences between the constants were insignificant (*K*=5.94×10^4 M^{-1} *vs.* 6.14×10^4 M^{-1}, Table 1).

According to the data in Table 1, we can consider that (**I**) binds to a single albumin site (n ≈1) presenting a moderate 1:1 affinity characterised by a constant of about 5×10^4 M^{-1}.

Although increasing temperature generally leads to an increase in the dynamic quenching process, we observe a decrease in the K_{SV} values, attesting to the predominance of static quenching. The decrease is more pronounced for K_{LB}, which characterizes only the static quenching process.

3.1.2. Thermodynamic analysis and the binding force

The ligand-binding process during protein–ligand complex formation is mainly governed by four types of weak, non-covalent forces including hydrogen bonds, van der Waals force, electrostatic, and hydrophobic interactions. To characterize the acting forces between coumarin-3-carboxylic acid and HSA/BSA, the thermodynamic parameters of the binding were estimated using the van't Hoff equation [30], considering that the enthalpy change (*ΔH^0*) does not vary significantly in the temperature range studied.

$$\ln K = \frac{-\Delta H^0}{RT} + \frac{\Delta S^0}{R} \quad (8)$$

where *K* is the binding constant at temperature *T,* and *R* is the gas constant. The enthalpy and entropy changes (*ΔH^0, ΔS^0*) are estimated from the plot ln *K vs. 1/T* (Eq. 8) allowing for calculations of the free energy change *(ΔG^0)*:

$$\Delta G^0 = \Delta H^0 - T\,\Delta S^0 \quad (9)$$

The values of *ΔH^0*, *ΔG^0*, and *ΔS^0* are included in Table 2. Ross and Subramanian [31] have characterized the sign and magnitude of the thermodynamic parameter associated with various individual kinds of interaction that may take place in protein association processes.

The negative values of both enthalpy and entropy for (**I**) and HSA indicate that the binding might involve both hydrogen bonding and van der Waals forces [32,33]. The large negative *ΔH^0* probably came mainly from

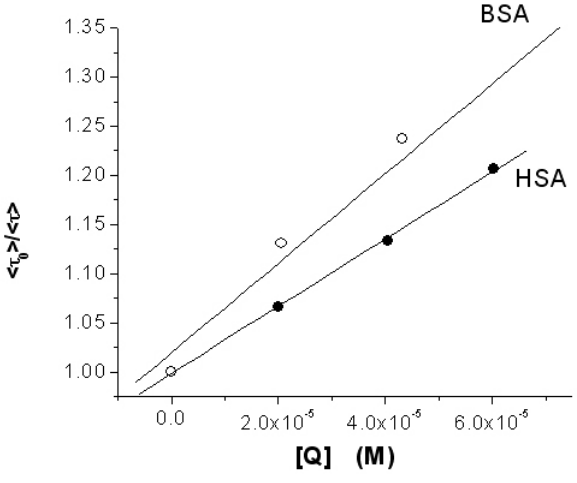

Figure 4. Time resolved Stern-Volmer plots for the dynamic quenching of HSA and BSA in the presence of (I), considering averaged τ values. [HSA] = [BSA] = 2.5×10^{-5} M; λ$_{ex}$= 304 nm.

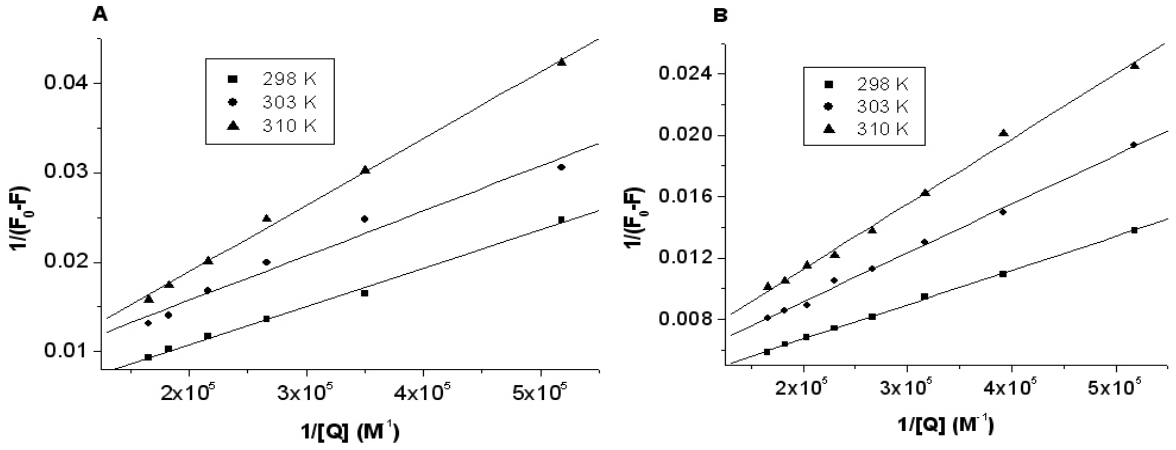

Figure 5. Lineweaver–Burk plots at different temperatures for A) HSA and B) for BSA. Experimental conditions as in Fig. 2.

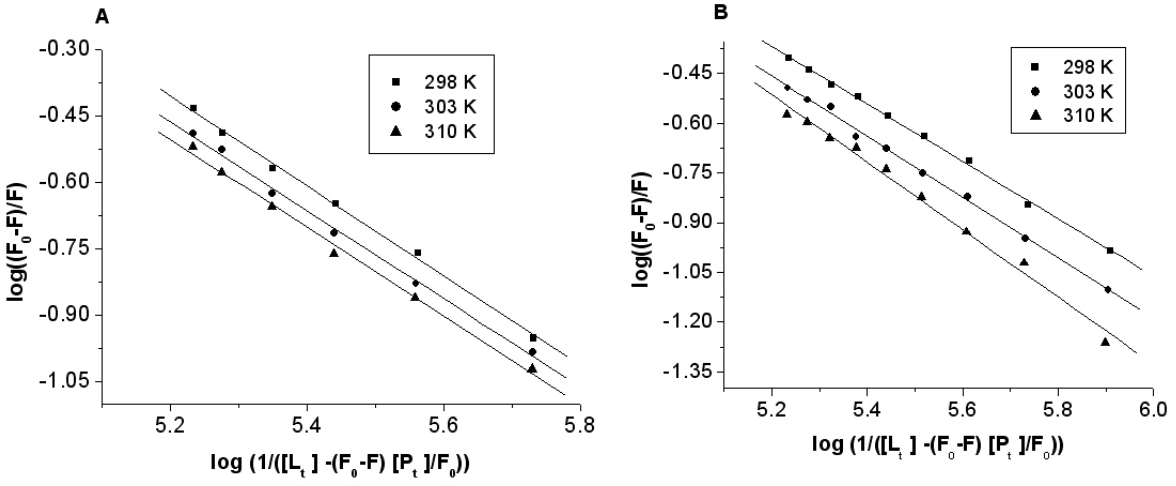

Figure 6. Fitting plot to Eq. 7 of A) HSA–(I) system ([HSA] = 0.75×10^{-6} M; λ_{ex} =286 nm; λ_{em} = 346 nm); R=0.998 (298 K); 0.997 (303 K); 0.997 (310 K); B) BSA–(I) system ([BSA] = 0.75×10^{-6} M; λ_{ex} =286 nm; λ_{em} = 339 nm); R=0.980 (298 K); 0.996 (303 K); 0.990 (310 K) for different temperatures.

Table 1. Averaged values of the Stern-Volmer constants (K_{SV}), of the Lineweaver-Burk constants (K_{LB}) and of binding parameters obtained by fitting the experimental data to Eq. 7.

	HSA			
	Eq. 1	Eq. 3	Eq. 7	
T (K)	$K_{SV}\times10^{-4}$ (M^{-1})	$K_{LB}\times10^{-4}$ (M^{-1})	n	$K\times10^{-4}$ (M^{-1})
298	5.77 ± 0.15	5.19 ± 1.20	1.01 ± 0.02	6.31 ± 0.23
303	5.46 ± 0.11	3.17 ± 1.11	0.99 ± 0.03	5.43 ± 0.29
310	4.97 ± 0.09	1.50 ± 0.75	0.99 ± 0.03	4.96 ± 0.28
	BSA			
T (K)	$K_{SV}\times10^{-4}$ (M^{-1})	$K_{LB}\times10^{-5}$ (M^{-1})	n	$K\times10^{-4}$ (M^{-1})
298	6.47 ± 0.14	1.01 ± 0.03	0.87 ± 0.01	5.94 ± 0.15
303	5.42 ± 0.13	0.82 ± 0.08	0.91 ± 0.02	4.99 ± 0.19
310	4.67 ± 0.13	0.69 ± 0.10	1.01 ± 0.04	4.96 ± 0.35

Table 2. The thermodynamic parameters of HSA/BSA- (I) obtained from binding constants obtained by fitting the experimental data to Eq. 3, at three different temperatures; pH = 7.4.

	T (K)	ΔG^0 (kJ mol^{-1})	ΔH^0 (kJ mol^{-1})*	ΔS^0 (J mol^{-1})*
HSA	298	-26.91	-79.68	-177.07
	303	-26.03		
	310	-24.79		
BSA	298	-19.67	-24.08	14.78
	303	-19.60		
	310	-19.50		

* *Statistical parameters of the fit, correlation coefficient (R) and standard deviation (SD): HSA) R=0.999; SD=0.029; BSA) R=0.990; SD=0.037;*

electrostatic interactions. In the case of BSA, the values ΔH^0 <0, ΔS^0 >0 reflect, according to literature data, a predominance of the electrostatic forces. Different signs for ΔH^0 and ΔS^0 were previously mentioned by Y. Sun *et al*. for HSA and BSA interaction with flavonoids [32].

3.1.3. Identification of binding sites

Both HSA and BSA consist of amino acids chains forming a single polypeptide, which contains three homologous α-helix domains (I–III). Each domain is divided into antiparallel six-helix and four sub-domains (A and B). Specific binding sites of albumins are located in hydrophobic cavities in sub-domains IIA and IIIA. Many ligands bind specifically to serum albumin (for example, warfarin for site I [32], ibuprofen for site II [35] and digitoxin for site III [36]). In order to identify the location of the (**I**) - binding site on HSA/BSA, warfarin and ibuprofen were used as site marker fluorescence probes for monitoring sites I and II of HSA/BSA, respectively [35,37,38]. The results are presented in Figs. 7 and 8.

The emission maximum for the HSA:warfarin 1:1 system is slightly shifted from the usual emission of the albumin at 343 nm to 349 nm. Addition of the ligand results in a gradual decrease of the HSA fluorescence together with a further red shift of the wavelength of the emission maximum from 349 to 361 nm (Fig. 7).

In the presence of ibuprofen, only a quenching of the emission without a significant shift of the band was observed (Fig. 8).

To facilitate the comparison of the influence of warfarin and ibuprofen on the binding of (**I**) to albumins, the binding constants in the presence of site markers were analyzed using Stern-Volmer method and Eq. 7. The corresponding constants are shown in Table 3.

For both albumins, in the presence of the markers, the 1:1 interaction is maintained, but the constants are differently modified.

For HSA, the results show that the binding constant decreased in the presence of warfarin, while a small influence was noted in the presence of ibuprofen. These results show that binding of (**I**) is perturbed by the presence of warfarin.

For BSA, the binding constant is modified more in the presence of ibuprofen (Table 3) than in the presence of warfarin, attesting to a more probable location of (**I**) in site II.

3.1.4. Synchronous fluorescence spectroscopy

Synchronous fluorescence spectra can provide information about the molecular environment in the vicinity of the fluorophore, in our case the tryptophan (Trp) and tyrosine (Tyr) residues. The Δλ values, *i.e.*, the difference between the excitation and emission wavelengths, that characterize the local environment around Trp and Tyr are

Δλ = 60 nm and Δλ = 15 nm, respectively [39]. The effect of (**I**) on HSA/BSA synchronous fluorescence spectroscopy is shown in Fig. 9A for HSA and Fig. 9B for BSA, at Δλ = 60 nm.

For both proteins it can be observed that for the d/p used, there was not a significant change in the band positions, but only a dramatic quenching in the emission intensities, about 65%. This led to the conclusion that the binding of (**I**) to the proteins did not produce a change in the polarity of the microenvironment of the Trp residues [40,41].

3.1.5. Energy transfer between coumarin-3-carboxylic acid and HSA/ BSA

The importance of the Förster resonance energy transfer in biochemistry is that the efficiency of transfer can be used to evaluate the distance between the ligand and the tryptophan residues responsible of the natural intrinsic fluorescence of the protein.

According to Förster's non-radiative energy transfer theory [42], the rate of energy transfer depends on: (i) the relative orientation of the donor and acceptor dipoles, (ii) the extent of overlap of the fluorescence emission

spectrum of the donor with the absorption spectrum of the acceptor, and (iii) the distance between the donor and the acceptor. The energy transfer effect is related not only to the distance between the acceptor and donor, but also to the critical energy transfer distance, R_0, as described in Eq. 10:

$$E = 1 - \frac{\tau}{\tau_0} = \frac{R_0^6}{R_0^6 + r^6} \quad (10)$$

where τ and τ_0 are the averaged protein lifetime in the presence and absence of (**I**), r is the distance between the donor and the acceptor and R_0 is the critical distance when the transfer efficiency is 50%:

$$R_0^6 = 8.8 \times 10^{-25} k^2 N^{-4} \Phi J \quad (11)$$

where k^2 is the spatial orientation factor of the dipole; N is the refractive index of the medium; Φ is the fluorescence quantum yield of the donor; and J is the overlap integral of the fluorescence emission spectrum of the donor and the absorption spectrum of the acceptor. J is given by:

$$J = \sum F(\lambda)\varepsilon(\lambda)\lambda^4 \Delta\lambda \,/\, \sum F(\lambda)\,\Delta\lambda \quad (12)$$

where $F(\lambda)$ is the fluorescence intensity of the fluorescent donor at wavelength λ and $\varepsilon(\lambda)$ is the molar absorption coefficient of the acceptor at wavelength λ. In the present case, k^2 = 2/3, N = 1.36 and Φ = 0.15. The efficiency was calculated from time resolved data.

The donor-to-acceptor distance, r <7 nm [43,44] indicated that the energy transfer from HSA/BSA to coumarin-3-carboxylic acid occurs with high possibility. Further, the value of r obtained in this way agrees very well with the literature value of substrate binding to serum albumin at site IIA [45,46]. The only aspect that should be noticed is that the BSA has two Trp residues, so that the donor-to-acceptor distance found may be in fact an average distance of the (**I**) from the two Trp residues.

3.2. Effect of the binding process on the protein conformation

To ascertain the possible influence of (**I**) binding on the secondary structure of HSA/BSA, CD measurements were performed in the presence of different concentrations of coumarin-3-carboxylic acid (Figs. 11A and 11B). CD spectra of HSA/BSA exhibit two negative bands in the ultraviolet region at 208 and 222 nm, which are characteristic for α-helix structure of proteins [47]. The binding of coumarin-3-carboxylic acid to proteins

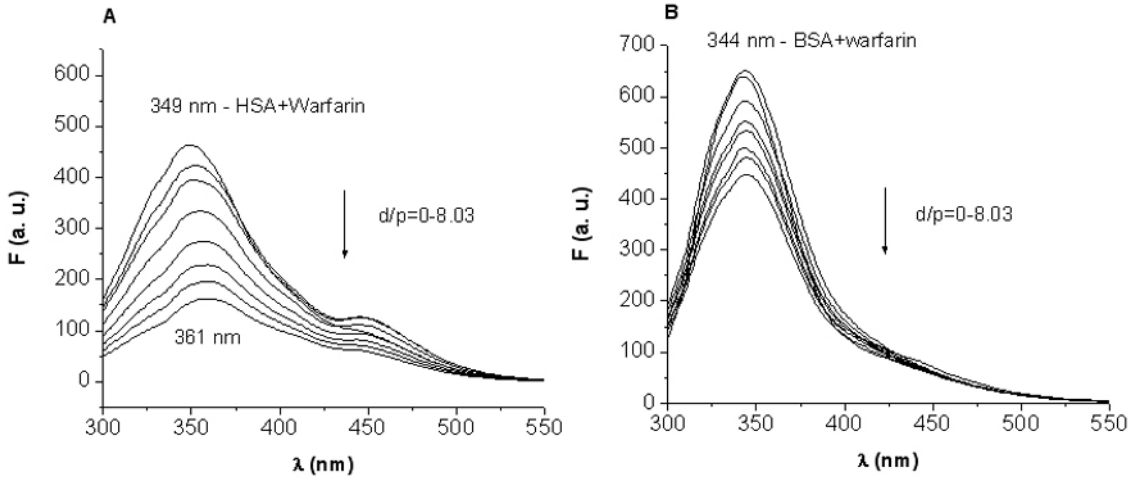

Figure 7. Effect of site marker warfarin to A) (I)-HSA system, [warfarin]=[HSA]=0.75×10^{-6} M; B) (I)-BSA system, [warfarin]=[BSA] = 0.75×10^{-6} M, T = 298 K, λ_{ex} = 286 nm, d/p=0-8.03.

Table 3. Effects of site probe on the Stern-Volmer constants, K_{SV} (M^{-1}) and on the binding constants, K (M^{-1}) of (I) to HSA and BSA; in brackets the correlation coefficients, R. Using Eq. 7, for all cases, as n ≈1 it was not included.

System	HSA		BSA	
	K_{SV}×10^{-4}	K×10^{-4} (Eq. 7)	K_{SV}×10^{-4}	K×10^{-4} (Eq. 7)
Blank	5.77 ± 0.15 (R= 0.996)	6.31 ± 0.23 (R=0.998)	6.47 ± 0.14 (R= 0.998)	5.94 ± 0.15 (R=0.990)
Warfarin	3.71 ± 0.07 (R= 0.997)	4.18 ± 0.09 (R=0.998)	5.13± 0.92 (R= 0.998)	4.52± 0.14 (R=0.996)
Ibuprofen	5.18 ± 0.09 (R= 0.997)	5.68 ± 0.10 (R=0.998)	4.03± 0.10 (R= 0.997)	3.18 ± 0.09 (R=0.998)

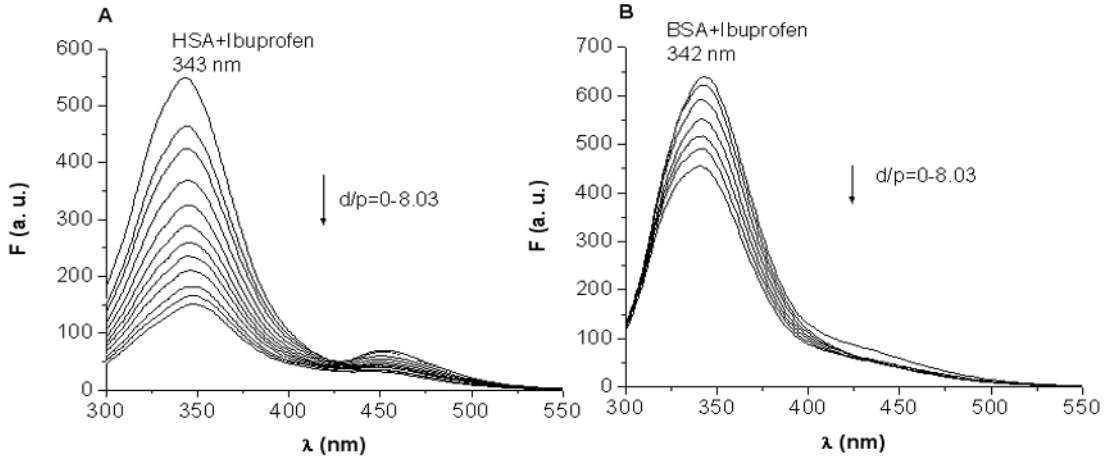

Figure 8. Effect of site marker ibuprofen to A) (I)-HSA system, [ibuprofen]=[HSA] =0.75×10^{-6} M; B) (I)-BSA system, [ibuprofen]=[BSA] =0.75×10^{-6} M, T = 298 K, λ_{ex} = 286 nm, d/p=0-8.03.

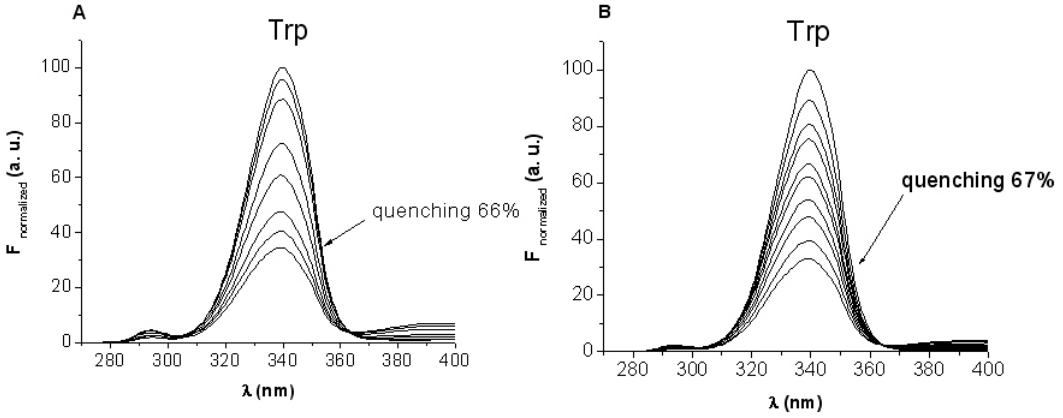

Figure 9. The effect of addition of (I) on the synchronous fluorescence spectrum at Δλ = 60 nm of A) HSA; B) BSA; T=298 K; pH=7.4;d/p=0-8.03.

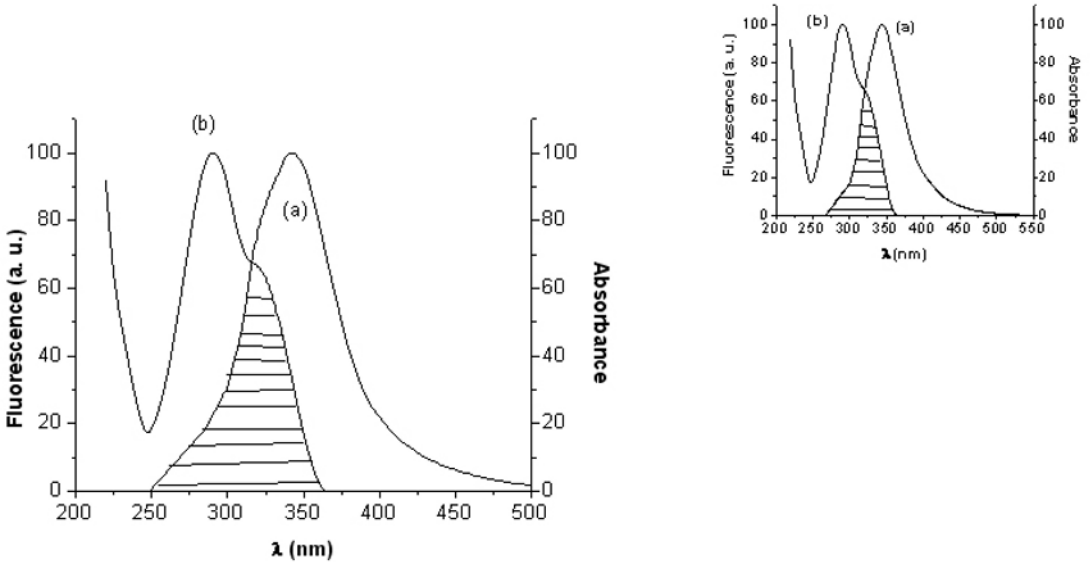

Figure 10. The overlap of (a) the fluorescence spectrum of HSA and (b) the absorption spectrum of (**I**). inset: The overlap of (a) the fluorescence spectrum of BSA and (b) the absorption spectrum of (**I**).

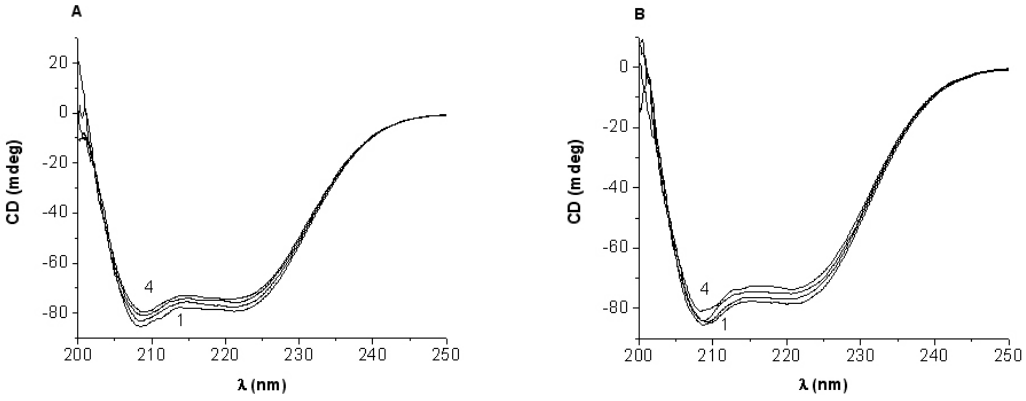

Figure 11. CD spectra of A) the HSA–(I) system; [HSA] = 0.75×10^{-6} M; B) the BSA–(**I**) system; [BSA] = 0.75×10^{-6} M; 1-4: d/p = 0; 1.32; 2.98; 4.86, respectively. T=298 K, pH =7.4.

Table 4. Energy transfer parameters: *J*, the overlap integral; *E*, the efficiency of energy transfer; R_0, the critical distance; r, the distance between the donor and the acceptor.

	J (cm^3 L mol $^{-1}$)	*E*	R_0 (nm)	*r* (nm)
HSA	4.25×10^{-15}	0.08	2.01	3.02
BSA	3.49×10^{-15}	0.12	1.95	2.72

Table 5. α- helix content of HSA and BSA at different dye/protein molar ratios.

d/p	(I)-HSA	(I)-BSA
0	52.90	53.26
1.32	52.01	52.84
4.86	51.31	52.05

caused a decrease in both bands, indicating a decrease of the α-helix content in proteins. The CD results were expressed in terms of mean residue ellipticity (*MRE*) [41] in deg cm^2 dmol^{-1} according to the following equation:

$$MRE = \theta_{obs}(mdgr)/\ 10\times n\times l\times C_p \qquad (13)$$

where θ_{obs} is the observed ellipticity from CD spectra in millidegrees, C_p is the molar concentration of the protein, *n* is the number of amino acid residues of the protein and *l* is the path length of the cell. The α-helix content of HSA/BSA is calculated from *MRE* values at 208 nm using the following equation [48]:

$$\alpha\text{- helix } \% = [(-MRE_{208} - 4000)/(33000-4000)] \times 100 \qquad (14)$$

where MRE_{208} is the observed MRE value at 208 nm, 4000 is the MRE value of random coil conformation, 33000 is the MRE value of a pure α-helix and β-form at 208 nm. From the above equation, the α-helix content of HSA/BSA was determined, the corresponding values being listed in Table 5.

The decrease of α-helix content is 1.59 % for HSA and 1.21 % for BSA, when the molar ratio of drug/protein is 4.86.

The decrease of the CD signal indicated that the binding of (**I**) to the two proteins induced some conformational changes in the latter, but the secondary structure of HSA / BSA remains predominantly α-helix.

4. Conclusions

In this work, the interaction of HSA/BSA with the coumarin-3-carboxylic acid − more precisely with the carboxylate ion, which is the dissociated species present at pH=7.4 − was studied by spectroscopic methods including steady-state and time-resolved fluorescence spectroscopy and CD spectra.

The analysis of the steady state fluorescence quenching data at several temperatures as compared to the results of the dynamic quenching shows that the quenching is mainly due to a static mechanism. The results obtained applying the Lineweaver-Burk treatment and a Scatchard-type equation show that for both proteins there is a 1:1 interaction with a binding constant of about 10^4 M^{-1} implying a moderate affinity. The competitive binding experiments in the presence of warfarin and ibuprofen as site markers indicate that in the case of HSA, coumarin-3-carboxylic acid binds with higher probability to the warfarin site, while for BSA, binding is predominantly to the ibuprofen site. The difference between the binding processes for the two proteins is also reflected by thermodynamic parameters attesting to the predominance of hydrogen bond and van der Waals forces in the case of HSA, and of electrostatic forces in the case of BSA.

The results of synchronous fluorescence spectroscopy suggested that binding between coumarin-3-carboxylic acid and the proteins did not lead to a change in the polarity of the microenvironment of the Trp residues. The analysis of the fluorescence quenching in terms of the Forster mechanism indicates a probable distance between the Trp214 and the ligand of about

3 nm. The changes in the HSA and BSA secondary structure monitored by circular dichroism are consistent with a slight decrease of the protein's α-helix content upon the binding process.

Acknowledgement

This work was financially supported by the grants 1644/2007 and 494/2008 from CNCSIS, Romania.

References

[1] A. Rieutord, P. Bourget, G. Torche, J.F. Zazzo, Int. J. Pharm. 119, 57 (1995)
[2] O. Bora, J. Pharm. Biopharm. 25, 63 (1997)
[3] F.P. Nicoletti, B.D. Howes, M. Fittipaldi, G. Fanali, M. Fasano, P. Ascenzi, G. Smulevich, J. Am. Chem. Soc. 130, 11677 (2008)
[4] O.K. Abou-Zied, O.I.K. Al-Shihi, J. Am. Chem. Soc. 130, 10793 (2008)
[5] T. Komatsu, R.M. Wang, P.A. Zunszain, S. Curry, E. Tsuchida, J. Am. Chem. Soc.128, 16297 (2006)
[6] J.R. Simard, P.A. Zunszain, C.E. Ha, J.S. Yang, N.V. Bhagavan, I. Petitpas, S. Curry, J. Hamilton, A Proc. Natl. Acad. Sci. U.S.A. 102, 17958 (2005)
[7] U. Kragh-Hansen, Pharmacol. Rev. 33, 17 (1981)
[8] S. Murata, M. Nishimura, S.Y. Matsuzaki, M. Tachiya, Chem. Phys. Lett. 219, 200 (1994)
[9] P. Suppan, Chem. Phys. Lett. 3, 94, 272 (1983)
[10] S. Nad, M. Kumbarkar, H. Pal, J. Phys. Chem. A 107, 4808 (2003)
[11] A. Kawski, Z. Natuforsch. 54A, 379 (1991)
[12] R. Giri, M.M. Bajaj, Curr. Sci. 62, 522 (1992)
[13] A. Samanth, W.E. Richard, J. Phys. Chem. A 104, 8972 (2000)
[14] H. Kolodziej, O. Kayser, H.J. Woerdenbag, W. Van Ulden, N. Pras, Naturforchung 52, 240 (1997)
[15] F.A. Jimenez-Orozco, J.A. Molina-Guarneros, N. Mendoza-Patino, F. Leon-Cedeno, B. Flores-Perez, E. Santos-Santos, J.J. Mandoki, Melanoma Res. 9, 243 (1999)
[16] G.J. Finn, B.S. Creaven, D.A. Egan, Melanoma Res. 11, 461 (2001)
[17] P. Laurin, M. Klich, C. Dupis-Hamelin, P. Mauvais, P. Lassaigne, A. Bonnefoy, B. Musicki, Bioorg. Med. Chem. Lett. 9, 2079 (1999)
[18] R.J.S. Hoult, M. Paya, Gen. Pharmacol. 27, 713 (1996)
[19] B. Thati, A. Noble, B. S. Creaven, M. Walsh, M. McCann, K. Kavanagh, M. Devereux, D. A. Egan, Cancer Letters 248, 321 (2007)
[20] A. Varlan, M. Hillebrand, Rev. Roum. Chim. 55(1), 69 (2010)
[21] A. Varlan, M. Hillebrand, Molecules 15, 3905 (2010)
[22] T. Otosu, E. Nishimoto, S. Yamashita, J. Biochem. 147, 191 (2010)
[23] J.R. Lakowicz, G. Weber, Biochemistry 12, 4161 (1973)
[24] M.R. Eftink, C.A. Ghiron, Anal. Biochem. 114, 199 (1981)
[25] J. Steinhardt, J. Krijn, J.G. Leidy, Biochemistry 10, 4005 (1971)
[26] H.X. Zhang, X. Huang, P. Mei, K.H. Li, C.N. Yan, J. Fluoresc. 16, 287 (2006)
[27] H.X. Zhang, X. Huang, P. Mei, S. Gao, J. Solution Chem. 37, 631 (2008)
[28] G. Scatchard, Ann. N.Y. Acad. Sci. 51, 660 (1949)
[29] M. van de Weert, J. Fluoresc, 20, 625 (2010)
[30] J.N. Tian, J.Q. Liu, W.Y. He, Z.D. Hu, X.J. Yao, X.G. Cheng, Biomacromolecules 5, 1956 (2004)
[31] D.P. Ross, S. Subramanian, Biochemistry 20, 3096 (1981)
[32] Y. Sun, H. Zhang, Y. Sun, Y. Zhang, H. Liu, J. Cheng, S. Bi, H. Zhang, J. Lumin. 130, 270 (2010)
[33] S. Ashoka, J. Seetharamappa, P.B. Kankagal, S.M.T. Shaikh, J. Lumin. 121, 179 (2006)
[34] M.A. Khan, S. Muzammil, J. Musarrat, Int. J. Biol. Macromol. 30, 243 (2002)
[35] G. Sudlow, D.J. Birkett, D.N. Wade, Mol. Pharmacol. 12,1052 (1976)
[36] I. Sjoholm, B. Ekman, A. Kober, I. Ljungstedt-Pahlman, B. Seiving, T. Sjodin, Mol. Pharmacol. 16, 767 (1979)
[37] G. Sudlow, D.J. Birkett, D.N. Wade, Mol. Pharmacol. 11, 824 (1975)
[38] S. Wanwimolruk, D.J. Birkett, P.M. Brooks, Mol. Pharmacol. 24, 458 (1983)
[39] U.K. Hansen, F. Hellec, B. de Foresta, M.L. Maire, J.V. Moller, Biophys. J. 80, 2898 (2001)
[40] K.R. Grigoryan, M.G. Aznauryan, N.A. Bagramyan, L.G. Gevorkyan, S.A. Markaryan, J. Appl. Spectrosc. 75(4), 593 (2008)
[41] J.-L. Yuan, Z. Iv, Z.-G. Liu, Z. Hu, G.-L. Zou, J. Photochem. Photobiol. A, 191, 104 (2007)
[42] S. Bi, D. Song, Y. Tian, X. Zhou, Z. Liu, H. Zhang, Spectrochim. Acta Part A 61, 629 (2005)
[43] Y.J. Hu, Y. Liu, J.B. Wang, X.H. Xiao, S.S. Qu, J. Pharm. Biomed. Anal. 36, 915 (2004)
[44] B. Valeur, J. C. Brochon, New trends in fluorescence spectroscopy (Springer Press, Berlin, 1999)

[45] S. Deepa, A.K. Mishra, J. Pharm. Biomed. Anal. 38, 556 (2005)
[46] J. Liu, J. Tian, J. Zhang, Z. Hu, Anal. Bioanal. Chem. 376, 864 (2003)
[47] P.B. Kandagal, S. Ashoka, J. Seetharamappa, S.M.T. Shaikh, Y. Jadegoud, O.B. Ijare, J. Pharm. Biomed. 41, 393 (2006)
[48] M.H. Rahman, T. Maruyama, T. Okaka, K. Yamasaki, M. Otagiri, Biochem. Pharmacol. 46, 1721 (1993)